

The calcium-activated chloride channel Anoctamin 1 contributes to the regulation of renal function

Diana Faria¹, Jason R. Rock², Ana M. Romao¹, Frank Schweda¹, Sascha Bandulik¹, Ralph Witzgall^{3,4}, Eberhard Schlatter⁵, Dirk Heitzmann⁵, Hermann Pavenstädt⁵, Edwin Herrmann⁶, Karl Kunzelmann^{1,7} and Rainer Schreiber^{1,7}

¹Universität Regensburg, Institute für Physiologie, Regensburg, Germany; ²Departments of Anatomy, Medicine and the Cardiovascular Research Institute, University California at San Francisco, San Francisco, California, USA; ³Universität Regensburg, Institut für Anatomie, Regensburg, Germany; ⁴Department of Internal Medicine D, Experimental Nephrology, Universitätsklinikum Münster, Albert-Schweitzer-Campus, Münster, Germany; ⁵Department of Internal Medicine D, Universitätsklinikum Münster, Albert-Schweitzer-Campus, Münster, Germany and ⁶Department of Urology, Universitätsklinikum Münster, Albert-Schweitzer-Campus, Münster, Germany

The role of calcium-activated chloride channels for renal function is unknown. By immunohistochemistry we demonstrate dominant expression of the recently identified calcium-activated chloride channels, Anoctamin 1 (Ano1, TMEM16A) in human and mouse proximal tubular epithelial (PTE) cells, with some expression in podocytes and other tubular segments. Ano1-null mice had proteinuria and numerous large reabsorption vesicles in PTE cells. Selective knockout of Ano1 in podocytes (Ano1^{-/-}/Nphs2-Cre) did not impair renal function, whereas tubular knockout in Ano1^{-/-}/Ksp-Cre mice increased urine protein excretion and decreased urine electrolyte concentrations. Purinergic stimulation activated calcium-dependent chloride currents in isolated proximal tubule epithelial cells from wild-type but not from Ano1^{-/-}/Ksp-Cre mice. Ano1 currents were activated by acidic pH, suggesting parallel stimulation of Ano1 chloride secretion with activation of the proton-ATPase. Lack of calcium-dependent chloride secretion in cells from Ano1^{-/-}/Ksp-Cre mice was paralleled by attenuated proton secretion and reduced endosomal acidification, which compromised proximal tubular albumin uptake. Tubular knockout of Ano1 enhanced serum renin and aldosterone concentrations, probably leading to enhanced compensatory distal tubular reabsorption, thus maintaining normal blood pressure levels. Thus, Ano1 has a role in proximal tubular proton secretion and protein reabsorption. The results correspond to regulation of the proton-ATPase by the Ano1-homolog Ist2 in yeast.

Kidney International (2014) **85**, 1369–1381; doi:10.1038/ki.2013.535; published online 29 January 2014

Correspondence: Karl Kunzelmann, Universität Regensburg, Institut für Physiologie, Universitätsstrasse 31, 93053 Regensburg, Germany.
E-mail: karl.kunzelmann@ur.de

⁷These two authors share senior authorship.

Received 13 May 2013; revised 16 October 2013; accepted 14 November 2013; published online 29 January 2014

KEYWORDS: Ano1; Anoctamin 1; Ca²⁺-activated Cl⁻ channels; H⁺-ATPase; renal proximal tubules; TMEM16A

Chloride channels function in renal tubular transport to maintain fluid, electrolyte, and acid-base balance. Numerous reports describe the existence of Ca²⁺-activated Cl⁻ channels (CaCC) in renal epithelial cells; however, their physiological role remains enigmatic.^{1–5} These channels have been suggested to contribute to Cl⁻ secretion and the growth of renal cysts in polycystic kidney disease.^{6–8} However, nothing is known about the physiological role of CaCC in the kidney. An increase in CaCC activity has been observed during renal inflammation and renal dedifferentiation, causing epithelial to mesenchymal transition.^{1,6} CaCC has now been identified as Anoctamin 1 (Ano1, TMEM16A).^{9–11} Ano1 has been shown to be essential for Ca²⁺-dependent Cl⁻ transport in a number of epithelial tissues, such as salivary and pancreatic glands, and in the respiratory epithelium.^{12–15} Ano1 is activated by stimulation of G-protein-coupled receptors, such as those for angiotensin or adenosine triphosphate (ATP).^{9,16} Interestingly, an upregulated purine metabolome was found in juvenile cystic mice, suggesting a role of Ano1 for renal cyst expansion.¹⁷

Identification of CaCC as Ano1 enabled us to examine the role of Ca²⁺-dependent Cl⁻ transport in the kidney. To that end, we generated conditional Ano1-knockout mice as the conventional knockout was lethal soon after birth.^{12,18} By selectively eliminating Ano1 expression in either mouse podocytes or tubular epithelial cells we unmask a role of Ano1 for proximal tubular proton secretion and protein reabsorption. Our results suggest a role of Ano1 for counterion movement necessary for effective H⁺ transport by the V-ATPase in human and mouse kidney.

RESULTS

Ano1 in human kidney

We analyzed expression of Ano1 in human kidney using reverse transcriptase-polymerase chain reaction (RT-PCR). Strong signals were found for Ano1, 3, 5, 6, 8, and 9 in both

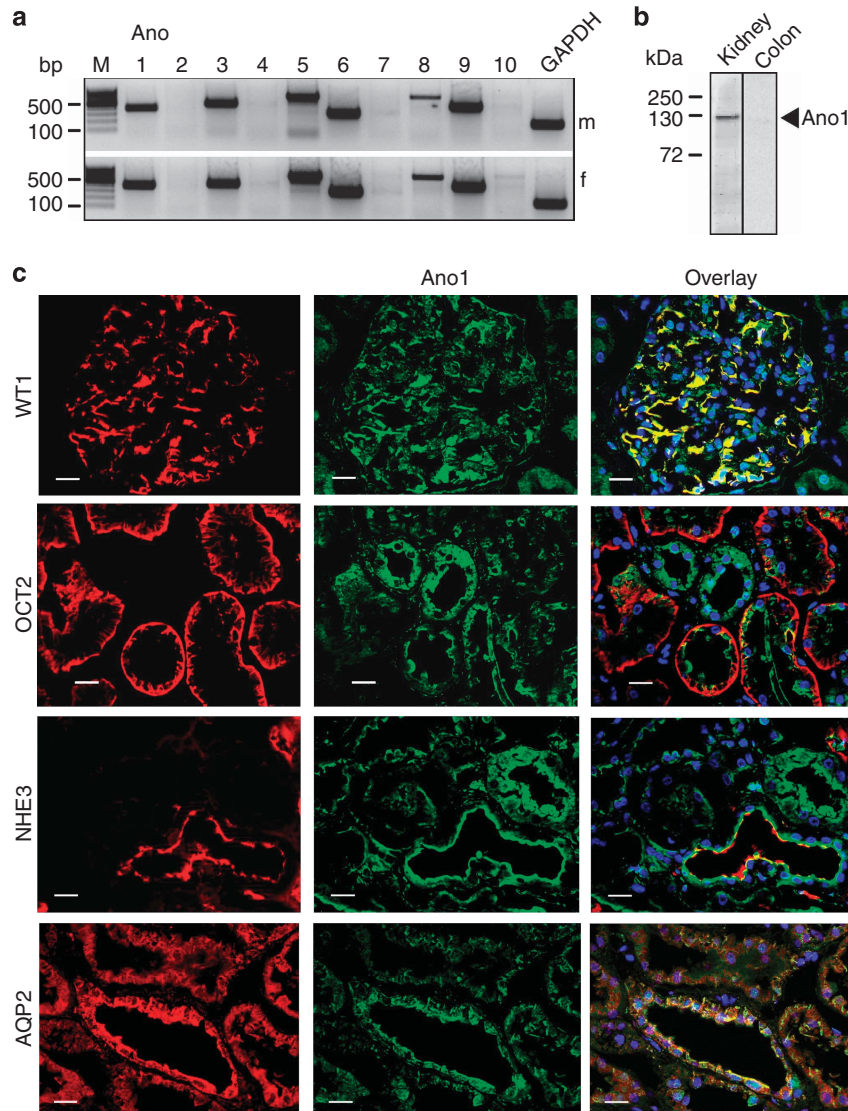


Figure 1 | Expression of anoctamins in human kidney. (a) Reverse transcriptase-polymerase chain reaction (RT-PCR) analysis of expression of Anoctamin 1 (Ano1)–10 in human male and female kidneys. (b) Western blot analysis of Ano1 protein expression in human kidney but not in colonic mucosa. (c) Immunohistochemistry of Ano1 in human kidney. WT1, podocyte Wilms’ tumor suppressor-1; OCT2, basolateral proximal tubular organic cation transporter 2; type 3 Na⁺/H⁺ exchanger, apical proximal tubular Na⁺/H⁺ exchanger type 3; AQP2, apical collecting duct water channel type 2. Scale bars, 20 μm. GAPDH, glyceraldehyde 3-phosphate dehydrogenase.

male and female kidneys. The Ano1 protein was detected in whole-kidney lysates, but not in human distal colon, which is known to lack Ca²⁺-activated Cl⁻ currents (Figure 1a and b, Supplementary Figure S1A online).¹⁹ Compared with whole-kidney lysates, Ano1 mRNA was less abundant in isolated human glomeruli, suggesting a predominant role of Ano1 for renal tubular transport rather than glomerular filtration (Supplementary Figure S1B online). Nevertheless, Ano1 was found to colocalize with podocyte Wilms’ tumor suppressor-1 in human glomeruli (Figure 1c). It was also found to be colocalized with the podocyte marker nephrin (Supplementary Figure S2A online). No staining was detected in the absence of primary antibodies (Supplementary Figure S2B online). Ano1 was most prominently present in the apical and probably the sub-apical compartments of

proximal tubular epithelial (PTE) cells as indicated by co-staining with the organic cation transporter OCT2, the type 3 Na⁺/H⁺ exchanger. Additional staining was found in principal epithelial cells of the collecting duct in which it colocalized with the apical water channel AQP2 (Figure 1c). Thus, Ano1 is predominantly expressed in the proximal tubule of human kidneys, with additional expression in podocytes and the collecting duct.

Expression of Ano1 in mouse kidney

We detected expression of mRNA and Ano1 protein in kidney lysates from wild-type (WT) animals but not from Ano1-knockout mice (Figure 2a and b).¹⁸ Ano1 expression was detected in glomeruli, in which it showed only weak colocalization with the podocyte marker synaptopodin (Figure 2c).

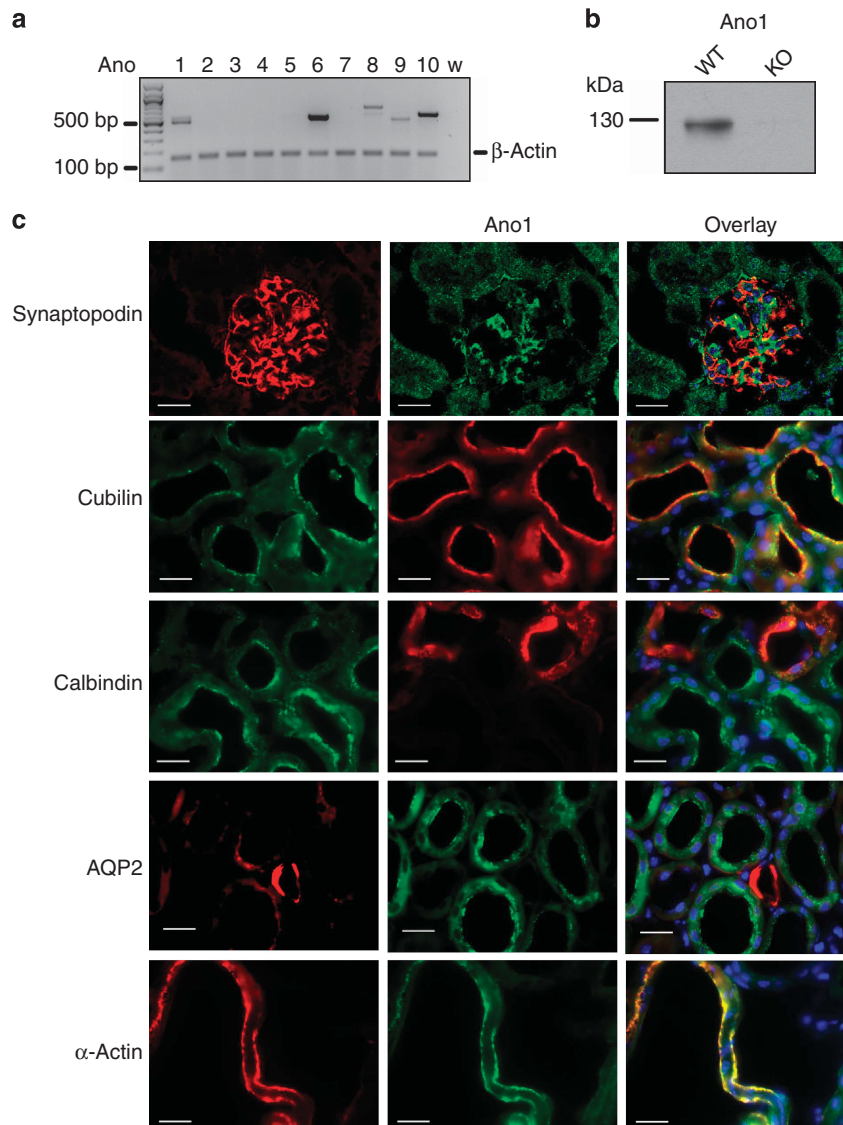


Figure 2 | Expression of Anoctamin in mouse kidney. (a) Multiplex-reverse transcriptase-polymerase chain reaction (RT-PCR) of Anoctamin 1 (Ano1)–10 and β -actin expression in mouse kidney. (b) Western blot analysis of whole-kidney lysates confirmed Ano1 protein expression in wild-type but not in Ano1-knockout mice. (c) Immunohistochemistry of Ano1 in mouse kidney. Synaptopodin, podocyte marker protein; cubilin, apical proximal tubular marker; calbindin, distal tubular marker; AQP2, apical collecting duct water channel type 2; α -actin, smooth muscle cell marker. Scale bars, 20 μ m.

Similar to human kidney, Ano1 was detected predominantly in the apical membrane of PTE cells, in which it colocalized with the protein cubilin and the V-ATPase (Figure 2c; Supplementary Figure S3A and D online). Ano1 did not colocalize with the distal tubular marker calbindin or the collecting duct marker AQP2, but with the smooth muscle cell marker α -actin (Figure 2c, Supplementary Figure S3C online). We therefore suggest a dominant role of Ano1 in the proximal tubules of both human and mouse kidneys, and possibly some function in glomerular podocytes.

Knockdown of Ano1 causes proteinuria

Lack of expression of Ano1 may compromise renal function. We therefore analyzed urine samples from Ano1-null mice,

which were severely ill.^{12,18} These animals only survive a few days after birth. Ano1 is broadly expressed in mouse and human tissues, particularly in epithelia, smooth muscles, and endocrine pancreas. Thus, there are numerous reasons why these animals die early, apart from non-stable airways due to cartilage malformation, as reported initially.¹⁸ At early postnatal stages, mice usually exhibit some proteinuria. However, we found that Ano1-null pups developed postnatal proteinuria more frequently (68.0%; $n=22$) when compared with WT littermates (13.6%; $n=22$) (Figure 3a). Proteinuria may be caused by defects in the glomerular filter or by impaired reabsorption of filtered proteins in the proximal tubule. Ultrastructural aspect of podocytes, for example, foot processes and filtration

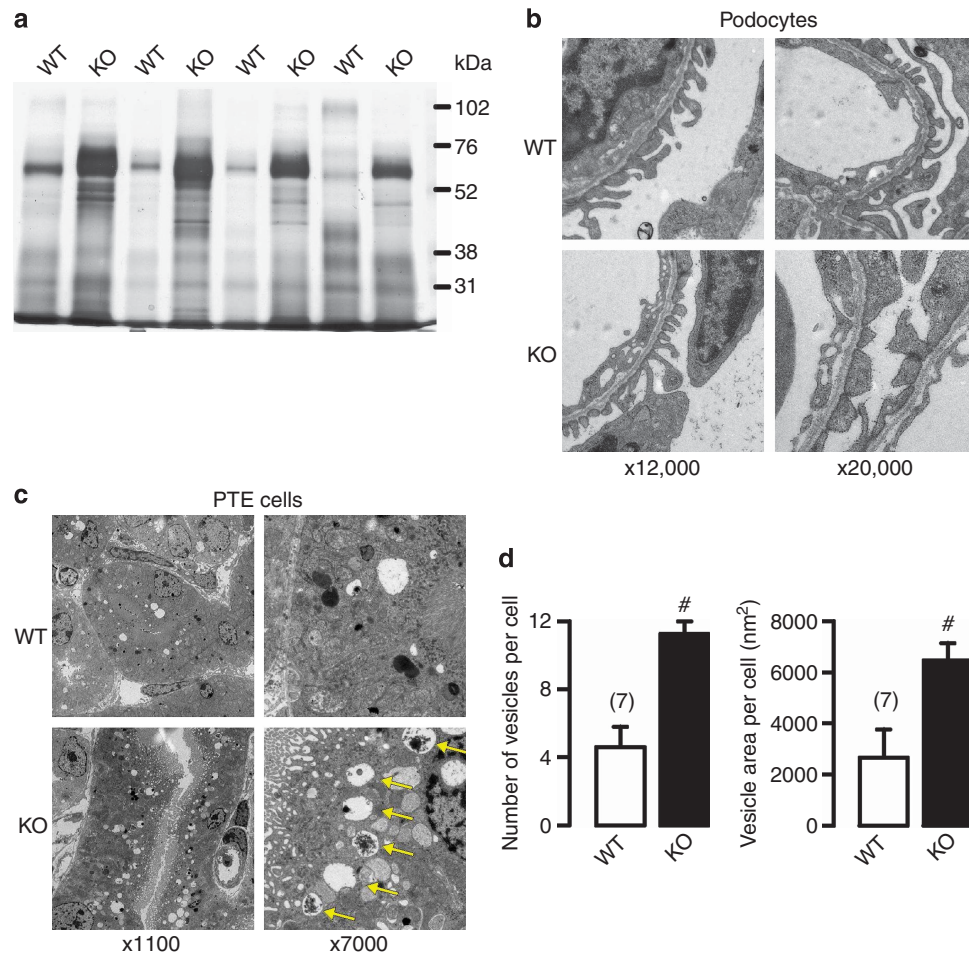


Figure 3 | Loss of Anoctamin 1 (Ano1) causes mild proteinuria. (a) Protein staining of urine samples from wild-type (WT) and Ano1-deficient mice (KO). 68% ($n = 22$) of Ano1-deficient mice demonstrate an increased protein excretion. (b) Electron microscopy of the glomerular filter and podocyte structure of WT and Ano1-knockout mice, without any ultrastructural difference. (c) Accumulation of intracellular vesicles (yellow arrows) in proximal tubular epithelial (PTE) cells from Ano1-knockout mice. (d) Quantification of number of vesicles per cell and vesicle area per cell in WT and Ano1-KO mice. Mean \pm s.e.m. (number of cells). #Significant difference (unpaired t-test).

membranes were not different in Ano1-null kidneys, whereas PTE cells of Ano1-deficient animals demonstrated accumulation of intracellular endosomal vesicles, which was not observed in cells from WT animals (Figure 3b, c and d). An increase in number and size of endosomal vesicles was also found in mice with a knockout of the $\alpha 4$ subunit of the V-ATPase.²⁰ To examine the renal function of Ano1 in more detail, we generated animals with a floxed Ano1 allele (c.f. Methods). These animals were crossed with mice demonstrating podocyte-specific expression (Ano1^{lox/lox}/Nphs2-Cre) or tubular epithelial cell-specific expression of Cre-recombinase (Ano1^{lox/lox}/Ksp-Cre).

Knockout of Ano1 in podocytes does not induce proteinuria

Crossing of Ano1^{lox/lox} with P2.5-Cre mice containing a Cre-recombinase expression cassette under the control of the *Nphs2* promoter (Ano1^{lox/lox}/Nphs2-Cre) leads to animals with specific knockout of Ano1 in podocytes.²¹ Cre-mediated

recombination of the *Ano1* gene was confirmed using PCR (Figure 4a). In addition, immunohistology showed reduced expression of Ano1 in glomeruli of Ano1^{lox/lox}/Nphs2-Cre mice (Figure 4b). No structural changes in the glomerular filter or podocytes were observed in these animals and reabsorption vesicles were not more frequent in PTE cells of Ano1^{lox/lox}/Nphs2-Cre animals (Figure 4c and d). Glomerular filtration rate and urine electrolyte excretion were normal; however, protein excretion was slightly, albeit not significantly, enhanced in Ano1^{lox/lox}/Nphs2-Cre mice (Figure 4e-g).

Tubular knockout of Ano1 impairs protein and electrolyte transport by PTE cells

To obtain tubular knockout of Ano1, Ano1^{lox/lox} mice were crossed with Ksp1.3-Cre mice that express the Cre-recombinase under the control of a *Cadherin 16* promoter (Ano1^{lox/lox}/Ksp-Cre).²² Cre-mediated recombination of the *Ano1* gene in PTE cells of Ano1^{lox/lox}/Ksp-Cre mice was demonstrated using PCR, western blots, and immunohistology

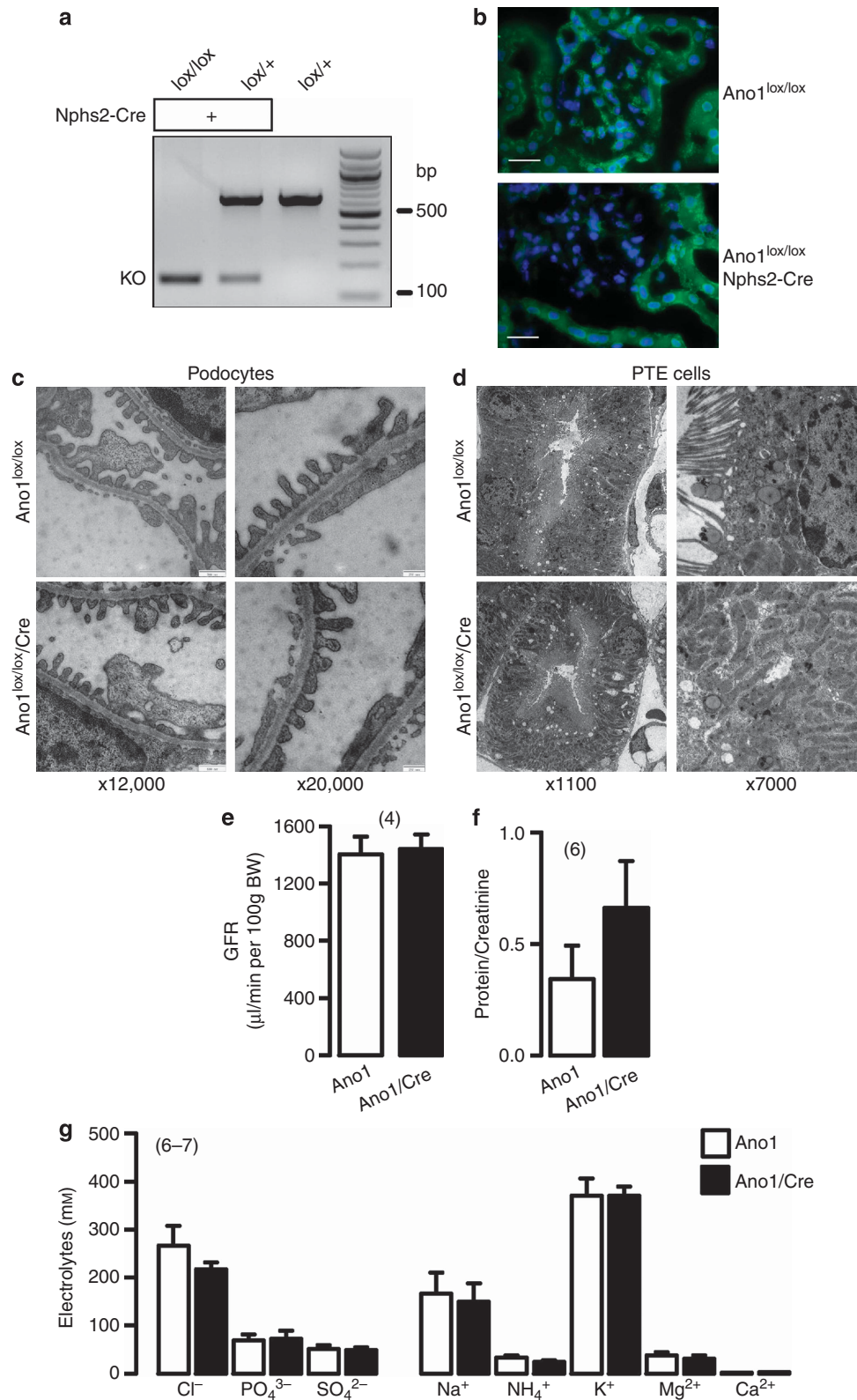
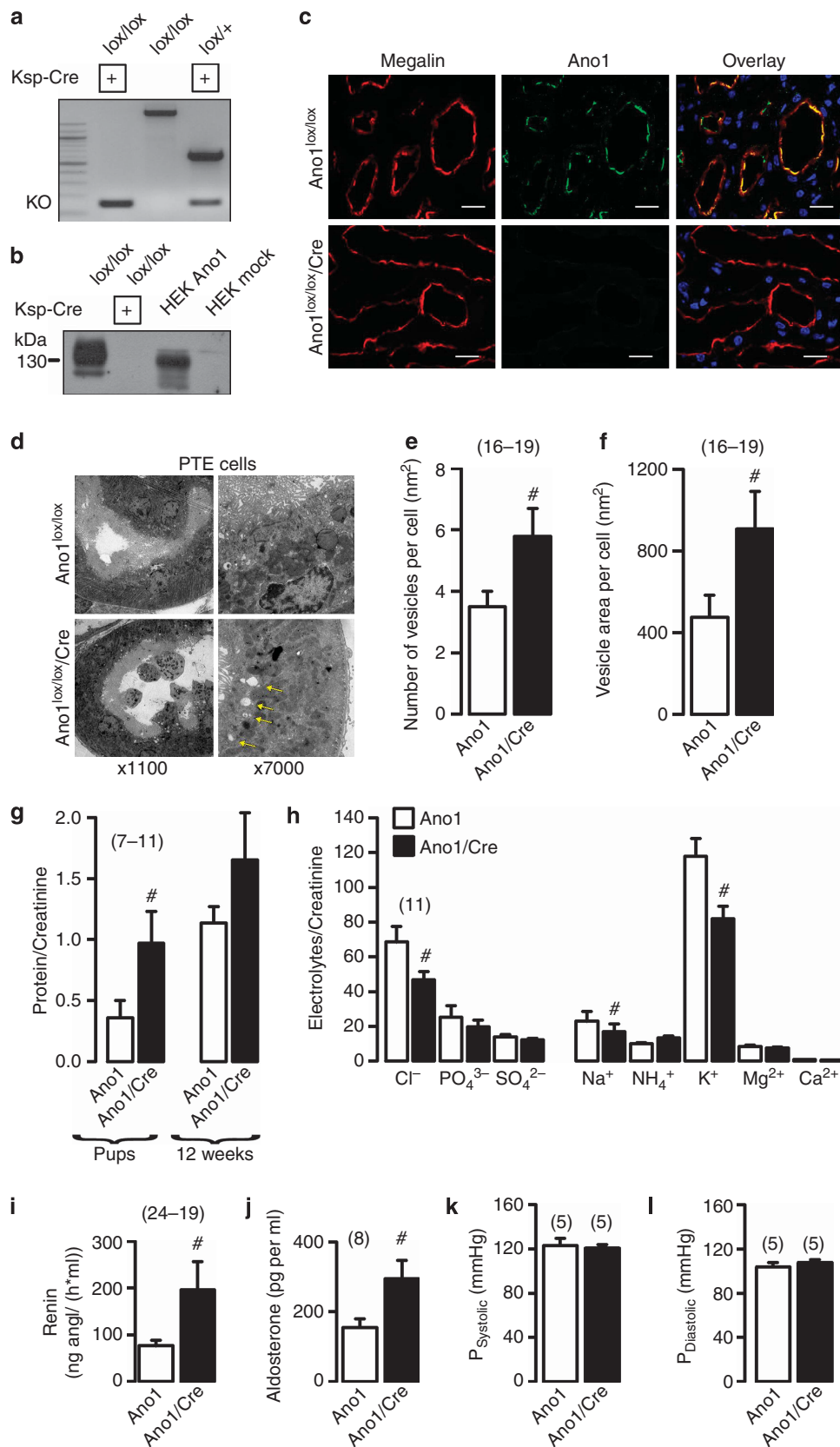


Figure 4 | Knockdown of Anoctamin 1 (Ano1) in podocytes does not change renal function. (a) Cre-mediated recombination of Ano1 in *Ano1^{lox/lox}/Nphs2-Cre* mice as demonstrated by reverse transcriptase-polymerase chain reaction (RT-PCR) (wild type: 635 bp; knockout: 150 bp). (b) Attenuated Ano1 expression in glomeruli of *Ano1^{lox/lox}/Nphs2-Cre* mice, as demonstrated by immunohistochemistry. (c and d) Electron microscopic images of podocytes and proximal tubular epithelial (PTE) cells from *Ano1^{lox/lox}/Nphs2-Cre* mice do not reveal any obvious structural changes. (e-g) Glomerular filtration rate, urine protein excretion, and electrolytes in *Ano1^{lox/lox}/Nphs2-Cre* mice were not different when compared with *Ano1^{lox/lox}* (wild-type) animals. All measurements were related to urine creatinine concentration (number of animals).



(Figure 5a–c). An accumulation of endosomal storage vesicles was observed at the apical pole of PTE cells (Figure 5d–f). As expected, glomerular filter and podocytes remained inconspicuous (Supplementary Figure S4 online). The protein excretion was enhanced in 1-day-old *Ano1*^{-/-} animals relative to WT animals; however, this difference faded as animals grew older (Figure 5g). Analysis of the type of proteinuria in *Ano1*^{-/-} mice indicated a predominant macro-albuminuria (Supplementary Figure S5A online). Interestingly, urine Cl⁻, Na⁺, and K⁺ concentrations were reduced in the tubular knockouts of 8- to 12-week-old animals, whereas both serum renin and aldosterone concentrations were enhanced. This suggests compensatory upregulation of reabsorption in the thick ascending limb and more distal tubular segments, resulting in normal systemic blood pressure (Figure 5h–l). Moreover, serum Na⁺ concentrations were not different between WT (146.6 ± 0.55 mmol/l; *n* = 3) and *Ano1*^{-/-} (144.86 ± 1.22 mmol/l; *n* = 3). The results suggest a defect in proximal tubular protein reabsorption in *Ano1*^{-/-} animals, that is not due to a change in

expression levels of megalin or tubulin, or the V-ATPase (Figure 6b and c). Moreover, as no evidence was found for an apical dyslocalization of the V-ATPase in tubular *Ano1*-knockout animals, we suggested a dysfunction of the V-ATPase in the absence of *Ano1* (Figure 6a).

Ano1 is a Ca²⁺-activated Cl⁻ channel in PTE cells

We further examined whether *Ano1* produces Ca²⁺-activated Cl⁻ currents in PTE cells. Isolated mouse PTE cells expressed *Ano1* mRNA and protein, along with typical marker proteins for PTE cells, such as megalin, cubilin, or SGLT1, but were negative for NKCC2 or AQP2 (Figure 7a and b). In Ussing chamber experiments under open-circuit conditions, apical application of the purinergic agonist ATP (10 μM) induced negative voltage deflections of the transepithelial voltage and increased the equivalent short-circuit current, indicating opening of apical Ca²⁺-activated Cl⁻ channels. Activation of these channels was inhibited by the CaCC inhibitor tannic acid (10 μM)²³ (Figure 7c and d). Activation of CaCC was also observed in fast whole-cell

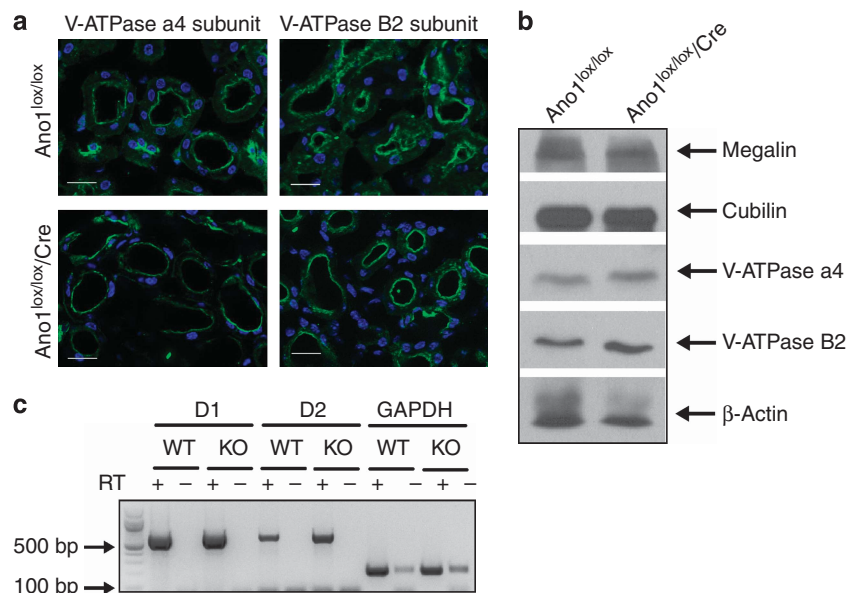


Figure 6 | Anoctamin 1 (*Ano1*) knockdown has no effect on expression and localization of V-ATPase, megalin, or cubilin.

(a) Immunolocalization of *Ano1* and two different V-ATPase subunits in the proximal tubule of wild-type (WT) and *Ano1*^{lox/lox}/Ksp-Cre mice. Bar = 50 μm. (b) Western blot analysis of megalin, cubilin, and two different V-ATPase subunits in proximal tubular epithelial cells from WT and *Ano1*^{lox/lox}/Ksp-Cre mice. (c) Reverse transcriptase-polymerase chain reaction (RT-PCR) analysis of expression of D1 and D2 subunits of the V-ATPase in proximal tubular epithelial cells from WT and *Ano1*^{lox/lox}/Ksp-Cre mice.

Figure 5 | Tubular knockdown of Anoctamin 1 (*Ano1*) compromises renal function. (a) Cre-mediated recombination of *Ano1* in *Ano1*^{lox/lox}/Ksp-Cre mice as demonstrated by reverse transcriptase-polymerase chain reaction (RT-PCR) (wild type: 635 bp, knockout: 150 bp). (b) Western blot analysis confirmed the absence of *Ano1* mRNA expression in primary proximal tubular epithelial (PTE) cells of *Ano1*^{lox/lox}/Ksp-Cre mice. *Ano1*-overexpressing HEK293 cells served as positive controls. (c) Immunohistochemistry demonstrates the absence of *Ano1* expression in megalin-positive proximal tubules of *Ano1*^{lox/lox}/Ksp-Cre mice. (d) Electron microscopy demonstrates the accumulation of intracellular vesicles (yellow arrows) in PTE cells from *Ano1*^{lox/lox}/Ksp-Cre mice. (e and f) Quantification of number of vesicles per cell and vesicle area per cell in *Ano1*^{lox/lox} and *Ano1*^{lox/lox}/Ksp-Cre mice indicates the accumulation of storage vesicles. (g) Urine protein/creatinine ratio of 1-day-old pups and 12-week-old *Ano1*^{lox/lox}/Ksp-Cre mice. (h) Urine electrolyte concentration related to creatinine in *Ano1*^{lox/lox}/Ksp-Cre and *Ano1*^{lox/lox} (WT) animals. (i and j) Serum renin activity and aldosterone concentrations were enhanced in 12-week-old *Ano1*^{lox/lox}/Ksp-Cre mice. (k and l) Systolic and diastolic pressures were identical in *Ano1*^{lox/lox}/Ksp-Cre mice and *Ano1*^{lox/lox} littermates. Mean ± s.e.m. (number of cells per animals). #Significant difference (unpaired *t*-test).

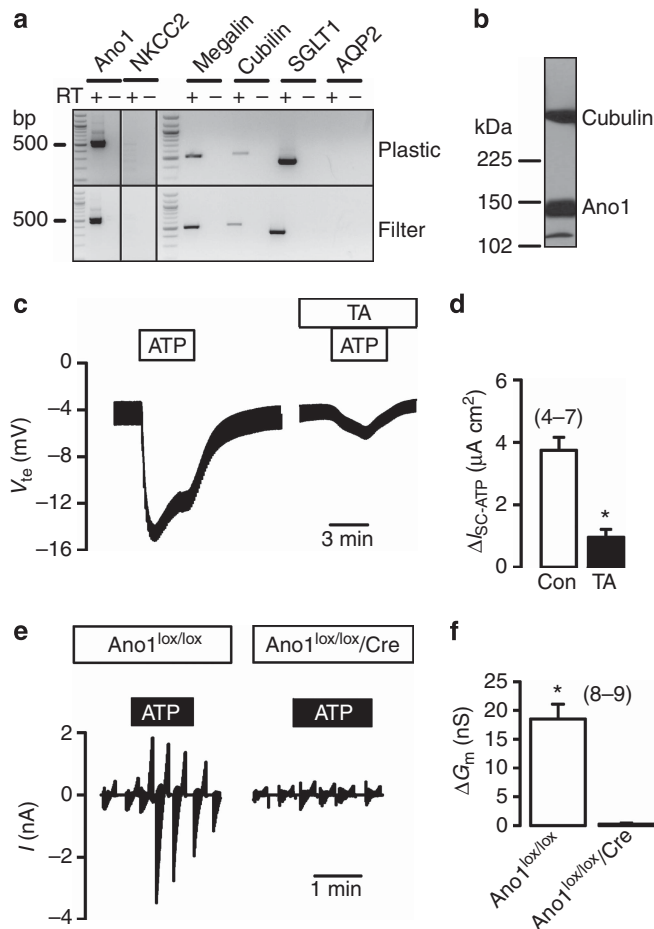


Figure 7 | Anoctamin 1 (Ano1) is a Ca^{2+} -activated Cl^- channel in proximal tubular epithelial (PTE) cells and missing in $Ano1^{lox/lox}/Ksp-Cre$ mice. (a) Reverse transcriptase-polymerase chain reaction (RT-PCR) analysis in primary PTE cells, grown on plastic surface or permeable supports, demonstrates expression of Ano1 along with the typical PTE proteins megalin, cubilin, and sodium glucose cotransporter-1 (SGLT1), but not sodium potassium chloride cotransporter NKCC2 and aquaporin-2 (AQP2). (b) Western blot analysis of primary PTE cells demonstrates expression of cubilin and Ano1. (c) Original recording of an Ussing chamber experiment with primary PTE cells grown on permeable supports. Adenosine triphosphate (ATP) (10 μ M) induced a large negative deflection of the transepithelial voltage indicating the activation of Cl^- secretion. Activation of Cl^- secretion was suppressed by tannic acid (TA; 10 μ M). (d) Summary of calculated ATP-induced equivalent short-circuit current (ΔI_{SC-ATP}) and inhibition by TA. (e) Original recordings of whole-cell currents from patch-clamp experiments, showing activation of currents by ATP in PTE cells from $Ano1^{lox/lox}/Ksp-Cre$, but not from $Ano1^{lox/lox}$ mice. Cells were voltage-clamped from -50 to $+100$ mV in steps of 10 mV. (f) Summary of the whole-cell conductances calculated from patch-clamp experiments. Mean \pm s.e.m. Number of cells per filter. *Significant difference (paired *t*-test).

patch-clamp experiments, upon stimulation of PTE cells with ATP (Figure 7e and f). In contrast, PTE cells from $Ano1^{lox/lox}/Cre$ mice lacking expression of Ano1 did not demonstrate any whole-cell current upon stimulation by ATP (Figure 7e and f). Moreover, membrane voltages of $Ano1$ -null cells were more hyperpolarized (-41.0 ± 4.6 mV; $n=9$) when compared with WT cells (-23.1 ± 4.0 mV; $n=9$), suggesting a basal activity of Ano1 even in the absence

of agonists. These results demonstrate that Ano1 forms a Ca^{2+} -activated Cl^- channel in the proximal tubular epithelium, which is absent in knockout cells.

Ano1 controls H^+ transport by the V-ATPase and uptake of albumin

We further examined the role of Ano1 in PTE cells. Whole-cell Cl^- currents were further activated by acidification of PTE cells from WT animals but not in $Ano1$ -null cells (Figure 8a). Cellular acidification was achieved by lowering bath pH in the presence of the protonophore carbonyl cyanide 3-chlorophenylhydrazone (10 μ M). Similar effects were observed in HEK293 cells overexpressing mouse Ano1 but not in mock-transfected cells (Figure 8b). Activation of Ano1 by protons suggests a role during proton secretion. In fact, earlier work demonstrated that proton secretion by the vacuolar H^+ -ATPase is Cl^- -dependent and can be activated by an increase in intracellular $[Ca^{2+}]_i$.²⁴ We found that cellular pH (pHi) was more acidic in the $Ano1^{lox/lox}/Ksp-Cre$ cells (Figure 8c).

pHi of PTE cells was acidified by changing the HCO_3^-/CO_2 -free bath solution to a ringer solution containing 25 mM HCO_3^- and 5% CO_2 , as the standard NH_3/NH_4^+ -pulse technique was not tolerated by the cells (Figure 8d and e).²⁵ Acidification by HCO_3^-/CO_2 -activated whole-cell Cl^- currents in $Ano1$ -expressing HEK293 cells, and the activation of Ano1 by low pH was not additive with the Ca^{2+} -dependent activation of Ano1 by 10 μ M ATP (Figure 8f). In contrast, acidification or ATP did not activate whole-cell currents in cells lacking Ano1 expression. In WT cells, pHi quickly recovered from acidification. Re-alkalinization could be inhibited by the H^+ -ATPase inhibitor bafilomycin (0.1 μ M). Although bafilomycin showed little effect in PTE cells from $Ano1^{lox/lox}/Cre$ mice, inhibition of the Na^+/H^+ exchanger by EIPA (10 μ M) largely impaired pH recovery in these cells (Figure 8d and e). This suggests that the proton pump is less active in PTE cells lacking Ano1 expression, which is compensated by upregulation of Na^+/H^+ exchange.

H^+ -ATPase activity is also essential for protein reabsorption and for acidification of endosomes in PTE cells. As $Ano1^{lox/lox}/Ksp-Cre$ pups showed signs of proteinuria, we measured fluorescein isothiocyanate (FITC)-albumin uptake in PTE cells. We found that uptake of FITC-albumin was significantly reduced in primary PTE cells lacking Ano1 expression (Figure 9a and b). In addition, pH in early and in late endosomes was less acidic in PTE cells from $Ano1/Ksp-Cre$ mice (Figure 9c). These results suggest Ano1 as a Cl^- shunt pathway for proximal tubular H^+ secretion and endosomal acidification induced by the vacuolar H^+ -ATPase.

DISCUSSION

Ano1 forms a Ca^{2+} -activated Cl^- bypass channel for H^+ extrusion by the H^+ -ATPase

We detected expression of Ano1 primarily in PTE cells of human and mouse kidney. The proximal tubule reabsorbs the largest fraction of filtered Na^+ along with water and

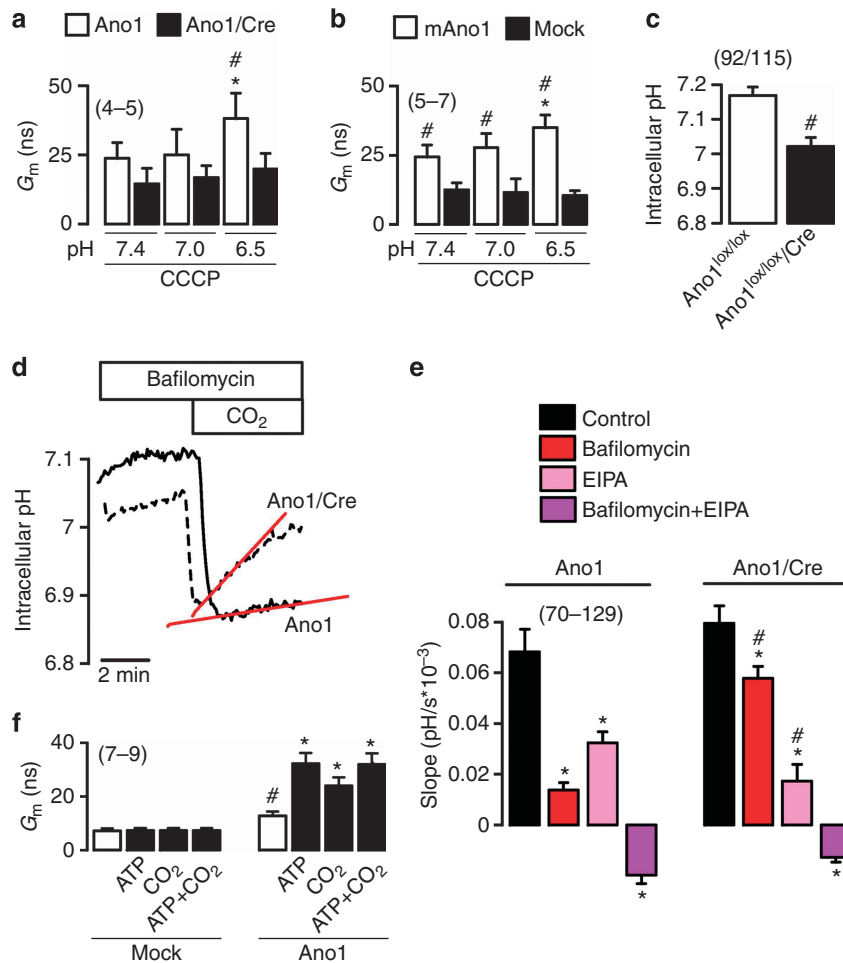


Figure 8 | H⁺-sensitive Anoctamin 1 (Ano1) supports the function of H⁺-ATPase in proximal tubelial (PTE) cells.

(a) Activation of Ano1 by acidic pH in the presence of the protonophore carbonyl cyanide 3-chlorophenylhydrazone (CCCP) (10 μ M), as detected in whole-cell patch-clamp experiment with primary PTE cells. No currents were activated in cells from Ano1^{lox/lox}/Ksp-Cre mice. (b) Activation of whole-cell currents by acidic pH in the presence of CCCP, in Ano1-overexpressing HEK293 cells but not in mock-transfected cells. (c) Intracellular pH (pHi) accessed by BCECF fluorescence. pHi was reduced in PTE cells from Ano1^{lox/lox}/Ksp-Cre mice. (d) Original recordings of pHi in the presence of the H⁺-ATPase inhibitor bafilomycin (0.1 μ M). Recovery of pHi from HCO₃⁻/CO₂-induced acidification was impaired in PTE cells from Ano1-expressing Ano1^{lox/lox} mice but not in cells from Ano1^{lox/lox}/Ksp-Cre mice. (e) Summary of pHi recovery after acid load (HCO₃⁻/CO₂). pHi recovery was measured as Δ pH/s and was identical in cells from Ano1^{lox/lox}/Ksp-Cre and Ano1^{lox/lox} mice under control conditions. pHi-recovery attenuated by bafilomycin or EIPA (10 μ M) and was even reversed by simultaneous application of both compounds. (f) Summary of whole-cell conductances in mock-transfected or Ano1-overexpressing HEK293 cells. Both ATP (10 μ M) and acidification by HCO₃⁻/CO₂-activated Ano1. Mean \pm s.e.m. (number of cells). *Significant difference when compared with control (paired *t*-test). #Significant difference when compared with mock (b and f) or Ano1^{lox/lox} (a, c and e) (unpaired *t*-test and analysis of variance (ANOVA)).

numerous substrates, including HCO₃⁻. Protons are secreted via apical Na⁺/H⁺ exchangers and vacuolar H⁺-ATPases. Translocation of H⁺ across the apical membrane of PTE cells by the vacuolar H⁺-ATPase is an electrogenic process that limits the transport activity of the pump.²⁶ Therefore, electrogenic H⁺ transport is probably paralleled by apical Cl⁻ channels that counterbalance charge movement.^{24,26–28}

Ano1 is a suitable candidate for a Cl⁻ bypass channel as: (i) it is expressed in the apical membrane of PTE cells, (ii) it supplies a baseline Cl⁻ conductance that is further activated by increase in intracellular Ca²⁺, (iii) it is potently inhibited by 5-nitro-2-(3-phenylpropylamino)-benzoate, which has been shown earlier to interfere with H⁺ extrusion by the

H⁺-ATPase,^{9,29} (iv) it has an anion permeability sequence that matches with that observed in earlier studies,³⁰ (v) knockdown of Ano1 acidifies PTE cells and (vi) impairs bafilomycin-sensitive H⁺ transport, and (vii) the yeast homolog of Ano1, Ist2, has been demonstrated recently to be essential for the function of the plasma membrane (PM) H⁺-ATPase.³¹

In yeast the H⁺-ATPase Pma1 pumps H⁺ across the PM and causes an electrochemical gradient that is used for secondary active uptake of nutrients such as amino acids.³² In contrast to Ano1, Ist2 is localized in the cortical endoplasmic reticulum in close proximity to the PM, where it may regulate Ca²⁺ signaling.³³ In PTE cells Ano1 is in the

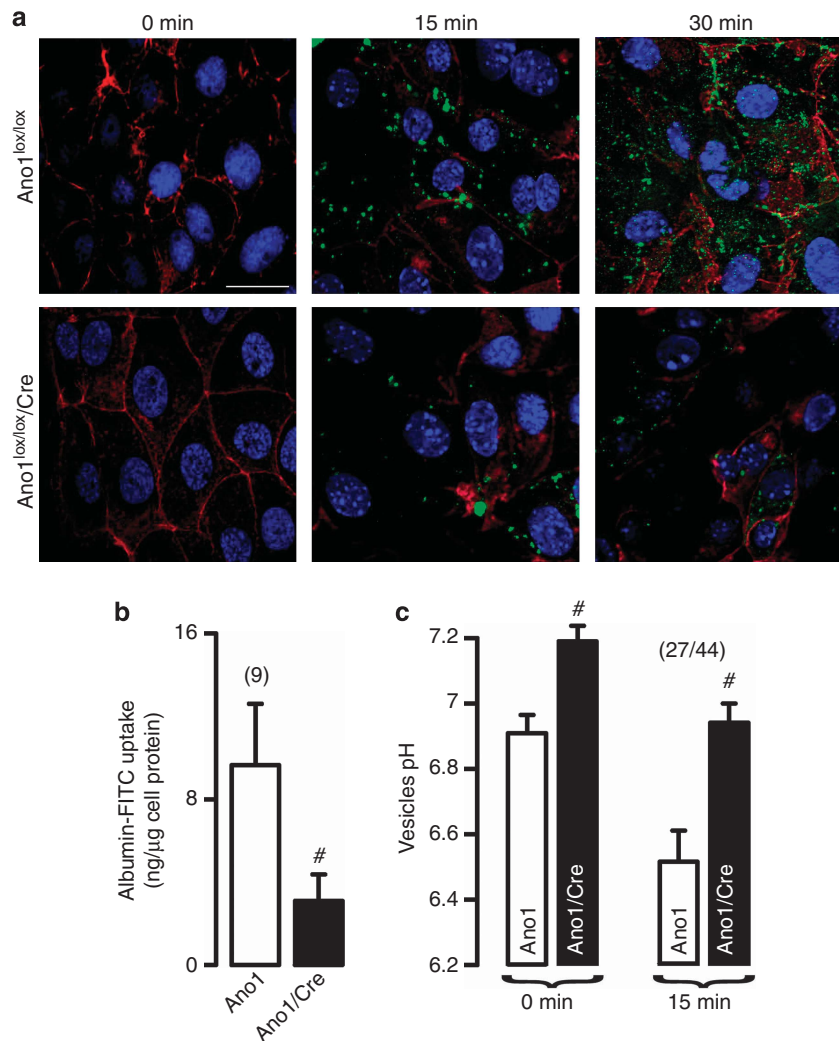


Figure 9 | Anoctamin 1 (Ano1) controls uptake of albumin and vesicular acidification. (a) Exposure of PTE cells from *Ano1^{lox/lox}* and *Ano1^{lox/lox}/Ksp-Cre* mice to fluorescein isothiocyanate (FITC)-albumin (5 mg/ml) for variable amounts of time. Green: FITC-albumin taken up by the cells. Blue: 4,6-diamidino-2-phenylindole (DAPI) stain of nuclei, Red: β -catenin membrane stain. (Scale bar 10 μ m.) (b) FITC-albumin uptake after a 30-min exposure was significantly reduced in PTE cells from *Ano1^{lox/lox}/Ksp-Cre* mice. (c) Acidification of vesicular pH in PTE cells, within 15 min after a 30-min loading with FITC-albumin (5 mg/ml) and subsequent washing of the cells. Acidification of vesicular pH was reduced in PTE cells from *Ano1^{lox/lox}/Ksp-Cre* mice. Mean \pm s.e.m. (number of cells). #Significant difference when compared with *Ano1^{lox/lox}* (unpaired t-test).

PM, in which it compensates the electrogenic effect of the H^+ -ATPase. Notably, in yeast cells lacking expression of Ist2, H^+ pumping was retrieved by the expression of Ano1.³¹

Flow-dependent co-regulation of H^+ -ATPase and Cl^- conductance

Anoctamin 1 is activated by stimulation of purinergic receptors and other receptors that couple to phospholipase C and intracellular Ca^{2+} (refs 9,16,34). Recent work demonstrates that an increase in tubular luminal flow stimulates the H^+ -ATPase in rabbit cortical collecting ducts.³⁵ This flow-induced H^+ transport was demonstrated to be Ca^{2+} -dependent.³⁵ Flow-induced ATP release, activation of apical purinergic receptors, and increase in intracellular Ca^{2+} have been shown earlier.³⁶ When we stimulated PTE cells with 10 μ M ATP, we found a significant increase in the rate of re-alkalinization from 0.013 ± 0.007 pH units/s ($-ATP$;

$n = 80$) to 0.035 ± 0.0013 pH units/s ($+ATP$; $n = 80$), suggesting that the concept of ATP—that is, flow-dependent regulation of H^+ secretion by the V-ATPase and activation of Ano1—may be likely. It is noteworthy that mechanosensitive Cl^- secretion by Ano1 has been demonstrated in the biliary epithelium.³⁷ Flow-induced increase in intracellular Ca^{2+} has been observed in renal and other ciliated epithelial cells.³⁶ It appears that flow-induced deflection of the primary cilium leads to an autocrine release of ATP and increase in intracellular Ca^{2+} , which may lead to parallel activation of the H^+ -ATPase and Ano1.³⁶ Intraluminal ATP concentrations in the proximal tubule reach levels up to 300 nM, which is sufficient to activate P2Y receptors.³⁸ Although data on the physiological regulation of Cl^- secretion by ATP in the renal tubular system are still limited, ATP and purinergic receptors have been shown to be involved in the pathogenesis of autosomal dominant polycystic kidney disease.^{7,8,39-41}

Activation of these receptors enhances dependent Cl^- secretion as well as cyst growth by the activation of extracellular regulated kinase.⁴²

Selective renal knockout of Ano1 causes a mild phenotype

The present data indicate an only mild phenotype in animals with a specific knockout of Ano1 in renal tubular cells. Despite reduced H^+ -ATPase function, urine pH was not different in the $\text{Ano1}^{\text{lox/lox}}/\text{Ksp-Cre}$ mice (6.9 ± 0.4 ; $n = 8$) compared with WT animals (6.9 ± 0.34 ; $n = 8$). Overall, the animals appeared somewhat dehydrated, and demonstrated an upregulated renin-angiotensin-aldosterone system, which appeared to normalize blood pressure and hematocrit ($\text{Ano1}^{+/+}$ 50.9 ± 1.4 ; $n = 8$ vs. $\text{Ano1}^{-/-}$ 51.9 ± 0.5 ; $n = 8$). The hematocrit was slightly, but not significantly, increased in $\text{Ano1}^{-/-}$ animals (41.7 ± 1.2 ; $n = 3$) when compared with WT animals (40.2 ± 0.6 ; $n = 4$).

Proteinuria was also mild and resolved as the animals grew older. A similar but much more pronounced phenotype was detected in a recent mouse model in which the $\alpha 4$ subunit of the V-ATPase was knocked out.²⁰ These animals developed a severe acidosis and demonstrated a proximal tubular dysfunction with defective endocytic trafficking, proteinuria, and accumulation of lysosomal material.²⁰ However, in contrast to the V-ATPase knockout, a number of anoctamin paralogs are expressed in renal epithelial cells, which are likely to compensate each other.¹⁶ Thus, blood gas analysis (serum pH, pCO_2 , HCO_3^- , BE) revealed no difference between WT and $\text{Ano1}^{-/-}$ animals (data not shown). The present data also suggest a role of Ano1 in the acidification of endosomal vesicles in PTE cells. This may complement the protein reabsorptive function of the endosomal chloride-proton exchanger ClC-5 ^{43,44} and CFTR.⁴⁵ Both Cl^- channels, in addition to other endogenous anoctamins, may compensate for the lack of Ano1 in $\text{Ano1}^{-/-}$ knockout animals. We propose that Ano1 may be particularly relevant during stimulation with Ca^{2+} -dependent secretagogues to facilitate endosomal acidification and to counterbalance electrogenic transport by the H^+ -ATPase.

MATERIALS AND METHODS

Mice

Ano1-knockout mice were a generous gift by Dr B. Harfe (University of Florida, Gainesville, USA) and J. Rock (University of California, San Francisco, USA). To generate the Ano1^{fl} allele $\text{Ano1}^{\text{Tm2}^{\text{JRR}}}$, a portion of BAC bMQ-379H21 (129S7/SvEv Brd-Hprt b-m2, AB2.2 ES cell DNA) was captured in a vector for recombineering as described earlier.⁴⁶ A loxp site was inserted upstream of the 161-bp exon 12 (the same exon replaced in $\text{Ano1}^{\text{tm1Bdh}}$). A PGK-neo cassette flanked by Fip recombinase target sites for positive selection in embryonic stem cells was inserted downstream of exon 12, followed by a second loxp site. The construct was linearized and electroporated into 129S6/SvEvTac ES cells by the Duke University Medical Center Transgenic Mouse Facility. Correctly targeted clones were identified by Southern blot and were transferred into C57BL/6 females. P2.5-Cre transgenic mice containing a Cre-expression cassette under the control of the *Nphs2* promoter were a generous

gift from Dr M. J. Möller (University of Aachen, Aachen, Germany).²¹ $\text{Ksp1.3}/\text{Cre}$ transgenic mice expressing Cre-recombinase under the control of the mouse cadherin 16 (*Cdh16*; *Ksp1.3*) promoter were a gift by Dr R. Warth (Department of Cell Biology, University of Regensburg, Germany).²²

Isolation of podocytes and PTE cells

Podocytes were isolated in digestion buffer containing collagenase 300 U/ml (Worthington, Lakewood, NJ, Type II), 1 mg/ml Pronase E (Sigma-Aldrich, Munich, Germany), and DNase I 50 U/ml (Applchem, Darmstadt, Germany). For the isolation of PTE cells, kidneys were dissected and proximal tubules were separated by a 45% Percoll (GE Healthcare, Munich, Germany) gradient centrifugation and kept in DMEM-F12 supplemented with 1% fetal bovine serum, 1% insulin/transferrin/selenium, 50 nM hydrocortisone, 5 nM T3 hormone, 5 nM EGF, and 1% penicillin/streptomycin. Tubule cells were grown in a humidified incubator at 37 °C with 5% CO_2 for 5–6 days.

Semi-quantitative RT-PCR, real-time PCR

Total RNA (2 μg) was reverse-transcribed and multiplex RT-PCR was performed using 0.5 μM primers (Supplementary Table S1 and S2 online). For real-time PCR, total RNA was isolated from primary PTE cells, reverse-transcribed using random primer and M-MLV reverse transcriptase (Promega, Mannheim, Germany), and analyzed in a Light Cycler 480 by using a Sybrgreen I PCR Kit (Roche Applied Science, Mannheim, Germany) and primers (Supplementary Table S3 online).

Immunohistochemistry and electron microscopy

Affinity purified polyclonal antiserum against mouse or human Ano1 was produced in rabbits immunized with (mouse) NHPSTTHPEAGDGPVPSYE (aa 957-976, C-terminus) or (human) YLKLKQQSPPDHEECVKKRQR (aa 688-708, third extracellular loop), coupled to keyhole limpet hemocyanin (Davids Biotechnologie, Regensburg, Germany). Mouse or human kidneys were fixed by perfusion with 4% paraformaldehyde and post-fixed in 0.5 mol/l sucrose and 4% paraformaldehyde solution. Cryosections of 5 μm were incubated in 0.1% sodium dodecyl sulfate for 5 min, washed with PBS, and blocked with 5% bovine serum albumin (BSA) and 0.04% Triton X-100 in PBS for 30 min. Sections were incubated with primary antibodies in 0.5% BSA and 0.04% Triton X-100 overnight at 4 °C and with Alexa Fluor 488-labeled donkey anti-rabbit IgG (Invitrogen, Darmstadt, Germany). Sections were counterstained with Hoe33342 (Sigma-Aldrich). Guinea pig anti-megalin was acquired from Dr F. Theilig, University Fribourg, Switzerland, goat anti-cubilin and anti-AQP2 were from Santa Cruz Biotechnology (Santa Cruz, Heidelberg, Germany), mouse anti-calbindin was from Swant (Bellinzona, Switzerland), and mouse anti- β -actin was from Immunotech (Marseille, France). Antibodies against V-ATPase A4 and B2 subunits were a generous gift from Carsten Wagner, University of Zurich, Switzerland. For co-staining in human kidneys, the following antibodies were used: mouse anti-hOCT2 (generous gift from Professor H. Koepsell, University Würzburg, Germany), mouse anti-Wilms' tumor suppressor-1 (Dako, Hamburg, Germany), goat anti-AQP2 (Santa Cruz Biotechnology), and mouse anti-type 3 Na^+/H^+ exchanger (Chemicon, Merck Millipore, Darmstadt, Germany). Immunofluorescence was detected using an Axiovert 200 microscope equipped with ApoTome and AxioVision (Zeiss, Germany). For electron microscopy, kidneys were perfusion-fixed and embedded in Epon according to standard

procedures. Thin sections (50 nm) were analyzed in a Zeiss EM 902 transmission electron microscope equipped with a cooled charge-coupled device digital camera (TRS, Moorenweis, Germany) as described earlier.³⁴

Measurement of intracellular and vesicular pH

Isolated PTE cells were incubated in ringer solution (mmol/l: NaCl 145; KH₂PO₄ 0.4; K₂HPO₄ 1.6; Glucose 5; MgCl₂ 1; Ca²⁺-Gluconat 1.3, Probenecid 5) containing 2 μM BCECF-AM (Life Technologies GmbH) and 0.02% Pluronic (Life Technologies GmbH, Darmstadt, Germany) for 60 min at 20 °C. To measure vesicular pH, cells were loaded with FITC-conjugated albumin (5 mg/ml, Sigma-Aldrich) for 30 min. Extracellular FITC-albumin was removed by dialyzing. For pH calibration, cells were superfused with a buffer of variable pH (5–7.4) containing nigericin (5 μmol/l). Excitation wavelengths of 490/440 and 500 nm were used for BCECF and FITC, respectively. Emission was recorded between 520 and 550 nm using a CoolSnap HQ (Visitron Systems, Puchheim, Germany).

Western blotting

Protein was isolated from human or mouse kidneys, primary PTE cells, or HEK293 cells using lysis buffer (50 mM Tris-HCl, 150 mM NaCl, 50 mM Tris, 100 mM DTT, 1% NP-40, 0.5% deoxycholate sodium) and 1% protease inhibitor cocktail (Roche Applied Science). Proteins were separated on 5 or 7.5% sodium dodecyl sulfate polyacrylamide gel and transferred to a polyvinylidene difluoride membrane (GE Healthcare) by wet transfer (Bio-Rad, Munich, Germany). Membranes were incubated overnight at 4 °C with a polyclonal rabbit anti-mouse Ano1 antibody (kindly provided by Dr B. Harfe, University of Florida, Gainesville, USA), rabbit anti-human Ano1 antibody (Cell Marque, Rocklin, CA), or goat anti-cubilin T16 antibody (Santa Cruz Biotechnology). Proteins were visualized using a horseradish peroxidase-conjugated secondary antibody and Super Signal west pico (Thermo Scientific, Schwerte, Germany).

Patch clamping and Ussing chamber

For patch clamping, cells were attached to collagen/fibronectin-coated glass coverslips, mounted on the stage of an inverted microscope (IM35, Zeiss), and kept at 37 °C. Patch pipettes were filled with a solution containing (mmol/l) NMDG 125, HCL 125, NaH₂PO₄ 1.2, Na₂HPO₄ 4.8, EGTA 1, Ca-gluconate 0.726, MgCl₂ 2.38, D-glucose 5, and ATP 3 at pH 7.2. Patch-clamp experiments were performed in fast whole-cell configuration as described recently.⁴⁷ Membrane conductance was calculated from the measured current (I) and V_c values according to Ohm's law. For Ussing chamber experiments, PTE cells were grown to confluence on permeable supports (Millipore, Darmstadt, Germany) and mounted into a perfused micro Ussing chamber. Experiments were performed under open-circuit conditions as described earlier.⁴⁷ R_{te} and equivalent short-circuit currents (I_{sc}) were calculated according to Ohm's law ($R_{te} = \Delta V_{te}/\Delta I$; $I_{sc} = V_{te}/R_{te}$).

Measurement of GFR and albumin uptake

Glomerular filtration rate was measured on awake animals as described earlier,⁴⁸ with the following modifications: FITC-sinistrin (5%) was dissolved in 0.9% NaCl, dialyzed, and sterilized by filtration. Blood samples were collected from the tail veins of FITC-sinistrin-injected mice at time points 0 (before injection) 3, 7, 10, 15, 35 and 55 min and were immediately diluted in HEPES to maintain pH at 7.4. Plasma samples were measured using

NanoDrop 3300 (Peqlab Biotechnologie, Erlangen, Germany). A standard FITC-sinistrin curve was applied to determine concentration. FITC-conjugated BSA was first dialyzed in 1000 ml ringer solution overnight at 4 °C. Uptake of FITC-conjugated BSA was determined as described earlier.⁴⁹

Analysis of urine samples, blood samples, and blood pressure

Mice were kept in metabolic cages for 24 h to examine diuresis. Spot urine was collected to analyze Cl⁻, PO₄³⁻, SO₄²⁻, Na⁺, NH₄⁺, K⁺ and creatinine using automated ionic chromatography (Isochratic dual ICS-1600-System and ICS-3000 Autosampler, Dionex/Thermo Fisher Scientific, Scoresby, Victoria, Australia). All measurements were related to the urine creatinine concentration. Protein concentrations were determined by the protein assay. Urine samples were normalized to creatinine analyzed using sodium dodecyl sulfate-polyacrylamide gel electrophoresis and silver staining. Blood was collected via submandibular puncture or retro-orbital sinus sampling. Aldosterone was measured using the IBL aldosterone ELISA kit (Hamburg, Germany). Renin was measured by generation of angiotensin I from homogenized kidneys in excess of renin substrate.⁵⁰ Glucose was assessed by glucose sticks (Accu-chek Comfort, Roche Applied Science). Urine pH was obtained using Neutralit pH 5–10 (Merck). Blood pressure was measured in conscious mice (*n* = 5 per group) using noninvasive tail-cuff manometry. Before taking measurements, animals were trained on three sequential days. The mean pressures were calculated from measurements taken on five sequential days.

Declaration

All animal experiments were approved by local authorities and were conducted according to the guidelines of the American Physiological Society and the German law for welfare of animals. Human kidney samples were obtained from tumor nephrectomy patients and written informed consent was received from participants before inclusion in the study. All procedures with human material were approved by the ethics commission of the Universitätsklinikum Münster, Germany.

DISCLOSURE

All the authors declared no competing interests.

ACKNOWLEDGMENTS

The work was supported by DFG SFB699/A7. We gratefully acknowledge the technical help by Helga Schmidt, Ute Neugebauer, Rita Schröter, Brigitte Wild, Julia Redekopf, and und Ines Tegmeier. We thank Dr Andrea Schreiber for excellent help with the isolation of proximal tubular epithelial cells and the metabolic caches. We appreciate the generous gifts of the Cre mice by Dr M. J. Möller (University of Aachen, Germany) and Professor Dr R. Warth (Universität Regensburg). The recommendations and help with the animal studies by Professor R. Warth is highly appreciated.

SUPPLEMENTARY MATERIAL

Figure S1. Expression of anoctamins in human kidney.

Figure S2. Expression of Ano1 in human kidney.

Figure S3. Expression of anoctamins in mouse kidney.

Figure S4. Ultrastructure of anoctamins in mouse kidney of Ano1^{lox/lox}/Ksp-Cre mice.

Figure S5. Effect of Ano1-knockout on expression of mRNA of other anoctamins.

Supplementary material is linked to the online version of the paper at <http://www.nature.com/ki>

REFERENCES

- AlDehni F, Spitzner M, Martins JR *et al.* Role of bestrophen for proliferation and in epithelial to mesenchymal transition. *J Am Soc Nephrol* 2009; **20**: 1556–1564.
- Boese SH, Aziz O, Simmons NL *et al.* Kinetics and regulation of a Ca²⁺-activated Cl⁻ conductance in mouse renal inner medullary collecting duct cells. *Am J Physiol Renal Physiol* 2004; **286**: F682–F692.
- Darvish N, Winaver J, Dagan D. Diverse modulations of chloride channels in renal proximal tubules. *Am J Physiol* 1994; **267**: F716–F724.
- Rubera I, Tauc M, Bidet M *et al.* Chloride currents in primary cultures of rabbit proximal and distal convoluted tubules. *Am J Physiol* 1998; **275**: F651–F663.
- Qu Z, Wei RW, Hartzell HC. Characterization of Ca²⁺-activated Cl⁻ currents in mouse kidney inner medullary collecting duct cells. *Am J Physiol Renal Physiol* 2003; **285**: F326–F335.
- Liu Y, Rajagopal M, Lee K *et al.* Prostaglandin E2 mediates proliferation and chloride secretion in ADPKD cystic renal epithelia. *Am J Physiol Renal Physiol* 2012; **303**: F1425–F1434.
- Hovater MB, Olteanu D, Welty EA *et al.* Purinergic signaling in the lumen of a normal nephron and in remodeled PKD encapsulated cysts. *Purinergic Signal* 2008; **4**: 109–124.
- Schwiebert EM, Wallace DP, Braunstein GM *et al.* Autocrine extracellular purinergic signaling in epithelial cells derived from polycystic kidneys. *Am J Physiol Renal Physiol* 2002; **282**: F763–F775.
- Yang YD, Cho H, Koo JY *et al.* TMEM16A confers receptor-activated calcium-dependent chloride conductance. *Nature* 2008; **455**: 1210–1215.
- Schroeder BC, Cheng T, Jan YN *et al.* Expression cloning of TMEM16A as a calcium-activated chloride channel subunit. *Cell* 2008; **134**: 1019–1029.
- Caputo A, Caci E, Ferrera L *et al.* TMEM16A, A membrane protein associated with calcium-dependent chloride channel activity. *Science* 2008; **322**: 590–594.
- Ousingsawat J, Martins JR, Schreiber R *et al.* Loss of TMEM16A causes a defect in epithelial Ca²⁺ dependent chloride transport. *J Biol Chem* 2009; **284**: 28698–28703.
- Rock JR, O'Neal WK, Gabriel SE *et al.* Transmembrane protein 16A (TMEM16A) is a Ca²⁺ regulated Cl⁻ secretory channel in mouse airways. *J Biol Chem* 2009; **284**: 14875–14880.
- Fischer H, Illek B, Sachs L *et al.* CFTR and Ca-activated Cl channels in primary cultures of human airway gland cells of serous or mucous phenotype. *Am J Physiol Lung Cell Mol Physiol* 2010; **299**: L585–L594.
- Huang F, Zhang H, Wu M *et al.* Calcium-activated chloride channel TMEM16A modulates mucin secretion and airway smooth muscle contraction. *Proc Natl Acad Sci USA* 2012; **109**: 16354–16359.
- Tian Y, Schreiber R, Kunzelmann K. Anoctamins are a family of Ca²⁺ activated Cl⁻ channels. *J Cell Sci* 2012; **125**: 4991–4998.
- Taylor SL, Ganti S, Bukanov NO *et al.* A metabolomics approach using juvenile cystic mice to identify urinary biomarkers and altered pathways in polycystic kidney disease. *Am J Physiol Renal Physiol* 2010; **298**: F909–F922.
- Rock JR, Futtner CR, Harfe BD. The transmembrane protein TMEM16A is required for normal development of the murine trachea. *Dev Biol* 2008; **321**: 141–149.
- Mall M, Bleich M, Greger R *et al.* Cholinergic ion secretion in human colon requires co-activation by cAMP. *Am J Physiol* 1998; **275**: G1274–G1281.
- Hennings JC, Picard N, Huebner AK *et al.* A mouse model for distal renal tubular acidosis reveals a previously unrecognized role of the V-ATPase a4 subunit in the proximal tubule. *EMBO Mol Med* 2012; **4**: 1057–1071.
- Moeller MJ, Sanden SK, Soofi A *et al.* Podocyte-specific expression of cre recombinase in transgenic mice. *Genesis* 2003; **35**: 39–42.
- Shao X, Somlo S, Igarashi P. Epithelial-specific Cre/lox recombination in the developing kidney and genitourinary tract. *J Am Soc Nephrol* 2002; **13**: 1837–1846.
- Namkung W, Thiagarajah JR, Phuan PW *et al.* Inhibition of Ca²⁺-activated Cl⁻ channels by gallotannins as a possible molecular basis for health benefits of red wine and green tea. *FASEB J* 2010; **24**: 4178–4186.
- Wagner CA, Giebisch G, Lang F *et al.* Angiotensin II stimulates vesicular H⁺-ATPase in rat proximal tubular cells. *Proc Natl Acad Sci USA* 1998; **95**: 9665–9668.
- Alpern RJ. Cell mechanisms of proximal tubule acidification. *Physiol Rev* 1990; **70**: 79–114.
- Wagner CA, Finberg KE, Breton S *et al.* Renal vacuolar H⁺-ATPase. *Physiol Rev* 2004; **84**: 1263–1314.
- Zimolo Z, Montrose MH, Murer H. H⁺ extrusion by an apical vacuolar-type H⁺-ATPase in rat renal proximal tubules. *J Membr Biol* 1992; **126**: 19–26.
- Malnic G, Geibel JP. Cell pH and H⁺ secretion by S3 segment of mammalian kidney: role of H⁺-ATPase and Cl⁻. *J Membr Biol* 2000; **178**: 115–125.
- Wagner CA, Mohebbi N, Uhlig U *et al.* Angiotensin II stimulates H⁺-ATPase activity in intercalated cells from isolated mouse connecting tubules and cortical collecting ducts. *Cell Physiol Biochem* 2011; **28**: 513–520.
- King N, Colledge WH, Ratcliff R *et al.* The intrinsic Cl⁻ conductance of mouse kidney cortex brush-border membrane vesicles is not related to CFTR. *Pflugers Arch* 1997; **434**: 575–580.
- Wolf W, Kilic A, Schrul B *et al.* Yeast Ist2 recruits the endoplasmic reticulum to the plasma membrane and creates a ribosome-free membrane microcompartment. *PLoS One* 2012; **7**: e39703.
- Arino J, Ramos J, Sychrova H. Alkali metal cation transport and homeostasis in yeasts. *Microbiol Mol Biol Rev* 2010; **74**: 95–120.
- Manford AG, Stefan CJ, Yuan HL *et al.* ER-to-plasma membrane tethering proteins regulate cell signaling and ER morphology. *Dev Cell* 2012; **23**: 1129–1140.
- Tian Y, Kongsuphol P, Hug MJ *et al.* Calmodulin-dependent activation of the epithelial calcium-dependent chloride channel TMEM16A. *FASEB J* 2011; **25**: 1058–1068.
- Liu W, Pastor-Soler NM, Schreck C *et al.* Luminal flow modulates H⁺-ATPase activity in the cortical collecting duct (CCD). *Am J Physiol Renal Physiol* 2012; **302**: F205–F215.
- Praetorius HA, Leipziger J. Primary cilium-dependent sensing of urinary flow and paracrine purinergic signaling. *Semin Cell Dev Biol* 2013; **24**: 3–10.
- Dutta AK, Woo K, Khimji AK *et al.* Mechanosensitive Cl⁻ secretion in biliary epithelium mediated through TMEM16A. *Am J Physiol Gastrointest Liver Physiol* 2012; **304**: G87–G98.
- Vekaria RM, Unwin RJ, Shirley DG *et al.* concentrations in rat renal tubules. *J Am Soc Nephrol*. 2006; **17**: 1841–1847.
- Hwang TH, Schwiebert EM, Guggino WB. Apical and basolateral ATP stimulates tracheal epithelial chloride secretion via multiple purinergic receptors. *Am J Physiol* 1996; **270**: C1611–C1623.
- Schwiebert EM, Zsembery A. Extracellular ATP as a signaling molecule for epithelial cells. *Biochim Biophys Acta* 2003; **1615**: 7–32.
- Xu C, Shmukler BE, Nishimura K *et al.* Attenuated, flow-induced ATP release contributes to absence of flow-sensitive, purinergic Ca²⁺ signaling in human ADPKD cyst epithelial cells. *Am J Physiol Renal Physiol* 2009; **296**: F1464–F1476.
- Turner CM, King BF, Srai KS *et al.* Antagonism of endogenous putative P2Y receptors reduces the growth of MDCK-derived cysts cultured *in vitro*. *Am J Physiol Renal Physiol* 2007; **292**: F15–F25.
- Piwon N, Gunther W, Schwake M *et al.* ClC-5 Cl⁻-channel disruption impairs endocytosis in a mouse model for Dent's disease. *Nature* 2000; **408**: 369–373.
- Novarino G, Weinert S, Rickheit G *et al.* Endosomal chloride-proton exchange rather than chloride conductance is crucial for renal endocytosis. *Science* 2010; **328**: 1398–1401.
- Jouret F, Bernard A, Hermans C *et al.* Cystic fibrosis is associated with a defect in apical receptor-mediated endocytosis in mouse and human kidney. *J Am Soc Nephrol* 2007; **18**: 707–718.
- Liu P, Jenkins NA, Copeland NG. A highly efficient recombineering-based method for generating conditional knockout mutations. *Genome Res* 2003; **13**: 476–484.
- Tian Y, Schreiber R, Wanitchakool P *et al.* Control of TMEM16A by INO-4995 and other inositolphosphates. *Br J Pharmacol* 2012; **168**: 253–265.
- Schmidt C, Hoehler K, Schweda F *et al.* Regulation of renal sodium transporters during severe inflammation. *J Am Soc Nephrol* 2007; **18**: 1072–1083.
- Schreiber A, Theilig F, Schweda F *et al.* Acute endotoxemia in mice induces downregulation of megalin and cubilin in the kidney. *Kidney Int* 2012; **82**: 53–59.
- AlDehni F, Tang T, Madsen K *et al.* Stimulation of renin secretion by catecholamines is dependent on adenylyl cyclases 5 and 6. *Hypertension* 2011; **57**: 460–468.